Induction of B Cell Hyperplasia in Simian Immunodeficiency Virus–infected Rhesus Macaques with the Simian Homologue of Kaposi's Sarcoma–associated Herpesvirus

By Scott W. Wong,*§ Eric P. Bergquam,* Ryan M. Swanson,* Felix W. Lee,* Stanley M. Shiigi,* Nancy A. Avery,* John W. Fanton,‡ and Michael K. Axthelm*

*From the *Division of Pathobiology and Immunology and the ‡Division of Animal Resources, Oregon Regional Primate Research Center, Beaverton, Oregon 97006; and the §Department of Molecular Microbiology and Immunology, Oregon Health Sciences University, Portland, Oregon 97201*

Summary

A simian homologue of Kaposi's sarcoma–associated herpesvirus (KSHV), the eighth human herpesvirus (HHV8), was isolated from a simian immunodeficiency virus (SIV)-infected rhesus macaque (*Macaca mulatta)* that developed a multicentric lymphoproliferative disorder (LPD). This simian rhadinovirus is genetically similar to a recently described rhesus rhadinovirus (RRV) (Desrosiers, R.C., V.G. Sasseville, S.C. Czajak, X. Zhang, K.G. Mansfield, A. Kaur, R.P. Johnson, A.A. Lackner, and J.U. Jung. 1997. *J. Virol.* 71:9764–9769) and is designated RRV 17577. RRV 17577 was experimentally inoculated into rhesus macaques with and without SIV_{mac239} infection to determine if RRV played a role in development of the LPD observed in the index case. In contrast to control animals inoculated with SIV_{mac239} or RRV alone, two animals coinfected with SIV_{mac239} and RRV 17577 developed hyperplastic LPD resembling the multicentric plasma cell variant of Castleman's disease, characterized by persistent angiofollicular lymphadenopathy, hepatomegaly, splenomegaly, and hypergammaglobulinemia. Hypergammaglobulinemia was associated with severe immune-mediated hemolytic anemia in one RRV/SIV-infected macaque. Both RRV/SIV-infected macaques exhibited persistent RRV viremia with little or no RRV-specific antibody response. The macaques inoculated with RRV alone displayed transient viremia followed by a vigorous anti-RRV antibody response and lacked evidence of LPD in peripheral blood and lymph nodes. Infectious RRV and RRV DNA were present in hyperplastic lymphoid tissues of the RRV/SIV-infected macaques, suggesting that lymphoid hyperplasia is associated with the high levels of replication. Thus, experimental RRV 17577 infection of SIV-infected rhesus macaques induces some of the hyperplastic B cell LPDs manifested in AIDS patients coinfected with KSHV.

Key words: B cell hyperplasia • simian immunodeficiency virus • rhesus rhadinovirus • lymphoproliferative disorders • nonhuman primate

Patients infected with HIV are at an increased risk for developing opportunistic infections and tumors, particularly Kaposi's sarcoma (KS)[1] and lymphoproliferative disorders (LPDs). Based on the epidemiology of KS among HIV patients, it was suggested that an infectious agent other than HIV must be involved in its pathogenesis (1). Recently, Chang et al. (2) isolated two short DNA fragments from a novel human herpesvirus that was present in DNA samples derived from KS lesions from patients with AIDS using representational differential analysis. This novel human rhadinovirus is referred to as KS-associated herpesvirus (KSHV), or human herpesvirus 8 (HHV8), and has been shown to be present in more than 90% of all KS lesions derived from both AIDS and non-AIDS patients (2–10). In addition to KS, KSHV infection has also been associated with primary effusion lymphoma (PEL) and multicentric

[1]*Abbreviations used in this paper:* BM, bone marrow; CPE, cytopathic effects; EBV, Epstein-Barr virus; HVS, *Herpesvirus saimiri*; KS, Kaposi's sarcoma; KSHV, KS-associated herpesvirus; LMP, latent membrane protein; LPDs, lymphoproliferative disorders; MCD, multicentric Castleman's disease; MIP, macrophage inflammatory protein; orfs, open reading frames; PEL, primary effusion lymphoma; RRV, rhesus rhadinovirus; SIV, simian immunodeficiency virus; TS, thymidylate synthase.

Castleman's disease (MCD) in AIDS patients. Both are unique B cell proliferative disorders that often occur in patients with AIDS-related KS (11–14).

Despite the accumulation of both molecular and serological data supporting the role of KSHV in KS, PEL, and MCD, understanding how KSHV is involved in these diseases is complicated by the absence of a relevant animal model. Attempts to induce KS or LPD by experimental KSHV infection of nonhuman primates previously infected with the simian immunodeficiency virus (SIV) have been unsuccessful, suggesting that KSHV, like human CMV, displays a strict species specificity (15). Although related gammaherpesviruses, namely *Herpesvirus saimiri* (HVS) and murine herpesvirus type 68, can cause LPD in some experimentally infected animals, they are inadequate models for KSHV pathogenesis, as they lack the KSHV-unique genes encoding the viral (v)IL-6 homologue, viral macrophage inflammatory proteins (vMIP-1), vIFN regulatory factor, and other rhadinovirus-unique genes that may contribute to pathogenesis (16, 17).

Recently, it was reported that rhesus macaques naturally harbor a rhadinovirus related to KSHV (18). Preliminary characterization of a 10.6–kilobase pair (kb) segment of the rhesus rhadinovirus (RRV) genome revealed a genetic organization similar to KSHV that included an IL-6–like gene in a position analogous to the IL-6–like gene encoded by KSHV. Despite the high incidence of RRV infection in captive rhesus macaques, no diseases have clearly been associated with RRV infection. However, analogous to humans infected with HIV and KSHV, animals infected with SIV or simian type D retrovirus (SRV) exhibit an increased frequency of LPD- and KS-like mesenchymoproliferative disorders than do immunocompetent animals, suggesting a role for infectious agents other than these immunosuppressive retroviruses (19–22). Recently, DNA sequences resembling those of KSHV were found in retroperitoneal fibromatosis tissue, a spindle cell tumor that is histologically similar to KS in SRV-infected macaques (23). Here we report the isolation of RRV strain 17577 from an SIV-infected rhesus macaque that developed a persistent multicentric LPD. SIV-infected rhesus macaques experimentally coinfected with RRV 17577 developed a hyperplastic B lymphocytic LPD resembling MCD, indicating that experimental RRV 17577 infection of SIV-infected rhesus macaques is a good model for the study of KSHV-associated B lymphocyte LPD manifested in AIDS patients.

Materials and Methods

Virus Isolation and Electron Microscopy. A bone marrow (BM) aspirate was collected in preservative-free ammonium heparin (1,000 U/ml) from a 2 y, 202-d-old captive-reared rhesus macaque 1 mo after experimental inoculation with a macrophage-tropic variant of SIV_{mac239}. The BM aspirate was dispersed, and isopynic gradient-purified (Ficoll-Paque; Pharmacia) BM mononuclear cells were seeded into T-25 culture flasks and grown in the presence of endothelial serum-free media (GIBCO BRL) supplemented with 10% fetal bovine serum, 1% l-glutamine, 1% penicillin/streptomycin/neomycin, and 30 μg/ml endothelial cell growth supplement (GIBCO BRL). Primary BM mononuclear cell cultures developed cytopathic effects (CPE) after 10–12 d and were rapidly frozen in liquid N_2 and thawed, and then supernatants were clarified by centrifugation and filtered through a 0.45-μM membrane. The filtered BM mononuclear cell culture extracts were inoculated on primary rhesus monkey fibroblast cultures (24). Fibroblast cultures developing CPE were scraped free into medium, pelleted at 400 *g*, washed in PBS, and suspended in cold Ito and Karnovsky's fixative (2.5% glutaraldehyde, 0.5% picric acid, 1.6% paraformaldehyde, 0.005% ruthenium red) in 0.1 M sodium cacodylate buffer, pH 7.4, for 2 h. Ito and Karnovsky's–fixed cells were washed in cacodylate buffer, postfixed in 1% OsO_4 and 0.8% $K_3Fe(Cn)_6$ in cacodylate buffer for 1 h, rinsed in distilled H_2O, and prestained in 2% aqueous uranyl acetate for 1 h. Fixed and prestained cells were dehydrated in a graded series of acetone, embedded in Epon 812 epoxy resin, polymerized at 60°C, and sectioned at 60 nm on an MT 5000 ultramicrotome. Copper grid–mounted sections were stained with lead citrate and uranyl acetate and viewed on a Phillips 300 electron microscope.

Virus Purification and Isolation of vDNA. Cell-free virus isolated from the primary BM mononuclear cell culture was serially passaged three times in primary rhesus fibroblasts to generate viral stocks, and the stocks were titered on primary rhesus fibroblasts before animal infection studies. For the isolation of vDNA, infected primary rhesus fibroblasts from two 850 cm^2 roller bottles were harvested and the cell debris removed by low speed centrifugation. The cell pellet was resuspended in culture medium, sonicated to release intracellular virus particles, and centrifuged to pellet cell debris. Virus was pelleted from supernatants by high speed centrifugation in a Beckman JA-14 rotor (Beckman Instruments, Inc.) for 1 h at 9,000 rpm and purified through a six-step sorbitol gradient ranging from 20 to 70% spun in a Beckman SW41 rotor for 2 h at 18,000 rpm. Gradient-purified virus was diluted in balanced buffered salts solution and pelleted through a 20% sorbitol cushion. The virus pellet was resuspended in Tris/EDTA buffer (TE; 10 mM Tris/HCl, pH 8.0, and 1 mM EDTA) and lysed in TE with 0.6% SDS and proteinase K (2 mg) at 37°C for 5 h. vDNA was isolated by $CsCl_2$ gradient centrifugation in a Beckman Ti 75 rotor at 38.4×10^3 rpm for 72 h, collected, and dialyzed against TE.

PCR Amplification of the Herpesvirus Polymerase Gene. PCR amplification of the herpesvirus polymerase gene was performed on purified vDNA using the following degenerated herpesvirus (HV) primers: HV-5, 5′-GCTCTAGATT(C,T)GA(C,T)AT(A,C,T)GA(A,G)TG(CT)-3′; and HV-6, 5′-GGATTCGG(G,A)AA(C,T)TC(G,A)TA(A,C,G,T)AC(A,C,G,T)TC-3′. The conditions for PCR amplification were as follows: 94°C for 2 min (1 cycle); 94°C for 1 min, 37°C for 1.5 min, 3-min ramp to 72°C, 72°C for 1.5 min (10 cycles); 94°C for 1 min, 50°C for 1 min, 72°C for 1.25 min (30 cycles); and 72°C extension for 10 min (1 cycle). Each PCR reaction used 0.1 μg of DNA, 50 pmol of each primer, 1 U of Vent polymerase, 40 μM of each deoxynucleotide triphosphate, 10 mM KCl, 10 mM Tris/HCl, pH 8.8, 10 mM $(NH_4)_2SO_4$, and 0.1% Triton X-100 in a final volume of 50 μl. Amplification was performed in a Perkin-Elmer 2400 Thermocycler. PCR products were run out on a 1% agarose gel; DNA fragments were isolated and restriction endonuclease digested with XbaI and EcoRI for cloning into pSP73 (Promega Corp.). Included in the degenerate PCR assay were DNA samples from rhesus CMV- and rhesus Epstein-Barr virus (EBV)-like lymphocryptovirus–infected cells (24, 25). DNA sequencing was performed

with Applied Biosystems (ABI) PRISM Dye Terminator Cycle Sequencing Ready Reaction Kits with AmpliTaq DNA polymerase as per the manufacturer's instructions. The DNA sequence was then determined on an ABI 373A sequencer in the Molecular Biology Core at the Oregon Regional Primate Research Center (ORPRC, Beaverton, OR). All plasmids were sequenced in both directions to verify DNA sequences. Open reading frames (orfs) were identified with MacVector (version 5.0; Oxford Molecular Group), and amino acid sequences were aligned by the CLUSTAL method (26) used with the MEGALIGN program provided with DNASTAR biocomputing software for the Macintosh.

Cloning and DNA Sequence Analysis of a Fragment Hybridizing to the KSHV Thymidylate Synthase Gene. Viral genomic DNA (5 μg) was restriction endonuclease digested with EcoRI, run out on a 1% agarose gel, and transferred to nitrocellulose. For use as a probe, the KSHV thymidylate synthase (TS) gene was generated by PCR amplification from DNA isolated from BCBL-1 cells (27) with oligonucleotide primers corresponding to a specific region of the KSHV genome encoding TS (nucleotides 20,236–20,650) (28) using standard PCR conditions. Immobilized vDNA was probed with random-primed, [^{32}P]dCTP-labeled KSHV TS for 16 h at 42°C. Hybridized membranes were then washed using conditions of moderate stringency (0.2× SSC and 0.1% SDS at 50°C) for 1 h, and bound probe was visualized by exposing DuPont-NEN reflection film to the washed membrane at −80°C with a DuPont-NEN reflection screen. The corresponding vDNA fragment found to hybridize was isolated and further digested with restriction endonuclease BamHI, which yielded a 3.4-kb fragment that was found to hybridize to the KSHV TS probe. This fragment was cloned into pSP73 and subjected to DNA sequence analysis as described above. Orfs were identified using MacVector software for the Macintosh, and the orfs were compared with SwissProt and PIR protein databases for homologous orfs with BLASTX. Alignments to identified proteins were generated either by the GAP program from the Wisconsin GCG analysis package (version 9.1; Oxford Molecular Group) or by the CLUSTAL program provided with the DNASTAR program. Sequences for RRV 17577 IL-6, TS, and MIP are available from EMBL/GenBank/DDBJ under accession number AF087411.

PCR Amplification for Detection of RRV DNA in Animal Samples. DNA extractions from peripheral blood and tissues were performed with a Puregene DNA isolation kit essentially as described by the manufacturer (Gentra Systems). PCR amplification for detecting the presence of the RRV genome was performed with the following oligonucleotide primers: vMIP-1, 5′-CCTATGGGCTCCATGAGC-3′; and vMIP-2, 5′-ATCGTCAATCAGGCTGCG-3′. PCR amplification for detecting the rhesus EBV genome was accomplished with oligonucleotide primers derived from published sequences of the latent membrane protein (LMP)-1 (29). PCR amplification of the rhesus β-globin gene was used as a control for the amount and quality of DNA used for each reaction (30). With the exception of β-globin, the conditions for PCR were 94°C for 2 min (1 cycle); 94°C for 0.5 min, 50°C for 0.5 min, 72°C for 0.5 min (30 cycles); and 72°C extension for 5 min (1 cycle). For the rhesus β-globin PCR, the annealing temperature was raised to 55°C. Each PCR reaction used 0.1 μg of total DNA, 50 pmol of each primer, 1 U of Vent polymerase, 40 μM of each deoxynucleotide triphosphate, 10 mM KCl, 10 mM Tris/HCl, pH 8.8, 10 mM $(NH_4)_2SO_4$, 2 mM $MgSO_4$, and 0.1% Triton X-100 in a final volume of 50 μl. The PCR reactions were run out on a 1% agarose gel, transferred to nitrocellulose, and probed with a [^{32}P]ATP-labeled oligonucleotide primer specific for vMIP (vMIP-3, 5′-ATATTAAACACTCGCCGC-3′), rhesus EBV LMP-1, or β-globin. Hybridizations were performed overnight at room temperature in 6× SSC, 0.1% SDS, and 10 mg/mL *Escherichia coli* tRNA. Southern blots were then washed with 2× SSC and 0.1% SDS twice at room temperature, followed by two washes for 1 h in 2× SSC and 0.1% SDS at 47°C (vMIP), 45°C (β-globin), or 52°C (rhesus EBV LMP-1), and bound probe was visualized by exposing DuPont-NEN reflection film to the washed membrane at −80°C.

Antibody Testing for RRV Infection. RRV 17577–infected cells were solubilized with 0.5% NP-40 and 1% sodium deoxycholate in PBS and clarified in a Beckman SW28 rotor at 23,500 rpm for 1 h at 4°C. The clarified supernatant was used as antigen for coating 96-well Maxisorp plates (500 ng/well; Nunc, Inc.). ELISAs were then performed essentially as described (31).

Experimental Infection and Evaluation of Animals. All aspects of the animal studies were performed according to institutional guidelines for animal care and use at the ORPRC. Rhesus monkeys (identification numbers 18483, 18503, 18540, and 18570) were inoculated intravenously with cell-free supernatants containing the equivalent of 5 ng of SIV_{mac} p27 prepared from Cos-1 cells transfected with a full length SIV_{mac239} molecular clone (32). Before experimental SIV inoculation, PBMCs from the four monkeys were prescreened for in vitro susceptibility to SIV_{mac239} infection essentially as described (33). 8 wk after SIV infection, animals 18483 and 18570 were inoculated intravenously with 5×10^6 PFU of RRV 17577. Two additional animals, 19092 and 19286, were also inoculated with 5×10^6 PFU of RRV 17577 as RRV-only controls. At sequential time points, animals were sedated with ketamine hydrochloride (10 mg/kg body weight) and given complete physical examinations. Venipunctures were performed, and EDTA- or preservative-free ammonium heparin–anticoagulated blood samples were collected and separated into plasma and PBMCs for analysis. Serial peripheral LN biopsies were performed, and PBMCs and dispersed LN mononuclear cells were cultured in 1640 medium (GIBCO BRL) supplemented with 20% fetal bovine serum, 1% l-glutamine, and 1% penicillin/streptomycin/neomycin to determine if continuously replicating or transformed cells were present. Plasma was monitored for SIV p27 during the first 4 wk after infection using the SIV p27 antigen capture ELISA (Coulter Immunology). Duplicate plating of 2×10^5 PBMCs or LN mononuclear cells on primary rhesus fibroblasts and PCR analysis of PBMCs and LN mononuclear cell DNA was used for RRV isolation and the detection of RRV DNA, respectively. Animals that became moribund were killed, and complete necropsies were performed. Tissues were snap-frozen in liquid N_2 for PCR analysis or fixed in neutral-buffered formalin, embedded in paraffin, sectioned, and stained with hematoxylin and eosin for light microscopy. Fresh PBMCs and dispersed mononuclear cells from lymphoid tissues were collected for leukocyte subset analyses, primary culture, and virus isolation via cocultivation with primary rhesus fibroblasts or cryopreserved for PCR analysis.

Alterations in subsets were monitored sequentially after experimental inoculations by FACS™ analysis (Becton Dickinson). T lymphocyte subsets were labeled with OKT4 (CD4; Ortho Diagnostic Systems, Inc.) and B9.11 (CD8, Coulter Immunology) mAbs. B lymphocytes were labeled with B-Ly-1 (CD20; Coulter Immunology) mAb. The CD23 and CD40 B cell activation markers were identified with EBVCS4 (provided by Dr. B. Sugden, University of Wisconsin, Madison, WI) and G28-5 (provided by Dr. J. Ledbetter, XCYTE Therapies, Seattle, WA) mAbs, respectively (34, 35). Total serum Ig (IgG and IgM) con-

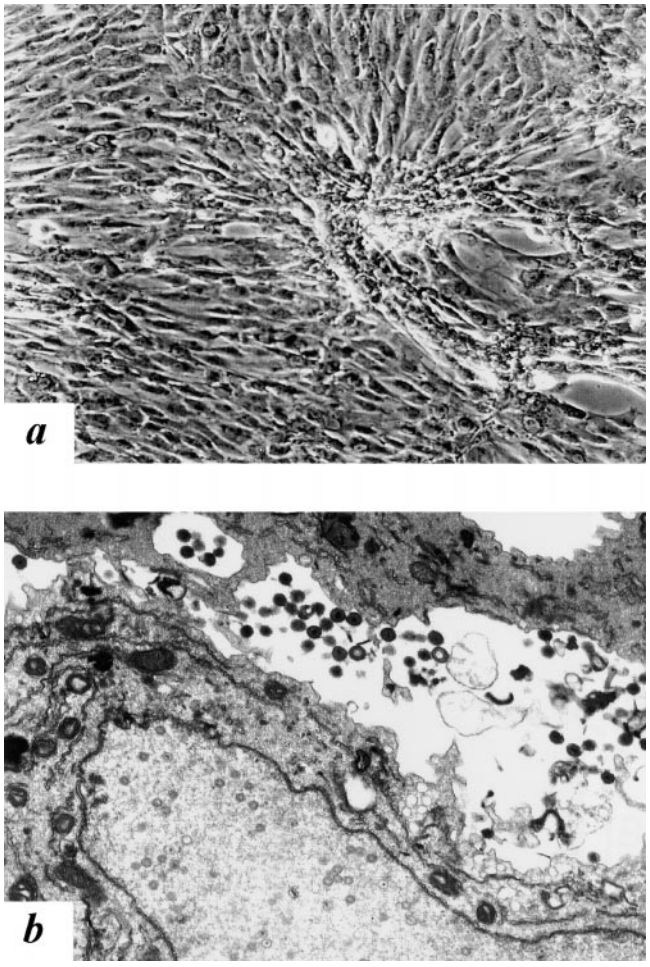

Figure 1. Productive infection of primary rhesus fibroblasts with herpesvirus. (a) Early stage CPE (magnification 100). (b) Electron micrograph of monolayers exhibiting CPE reveals immature herpesvirus particles in the nucleus and mature enveloped viral particles in the extracellular space.

centrations and κ and λ light ratios in total serum Ig were determined by nephelometry, and the Coombs' test (direct antiglobulin) was performed to determine if hemolytic anemia in one of the animals was immune mediated (Quest Diagnostics, Inc.).

Results

Isolation and Characterization of RRV Strain 17577. Primary cell cultures established with BM mononuclear cells from macaque 17577 developed CPE in the fibroblast-like adherent cells after 10–12 d in culture and were harvested for passage. Primary rhesus monkey fibroblast cultures were inoculated with filtered extracts from the primary BM cultures. 10–12 d after inoculation, fibroblast cultures developed CPE characterized by granular focal lesions followed by cell rounding and sloughing that generated holes in the monolayer (Fig. 1 a). Transmission electron microscopic examination of the infected fibroblasts revealed 150–200-nm virus particles with characteristic dense cores resembling herpesviruses in the extracellular spaces as well as immature and mature virus particles in the nuclei and cytoplasm, respectively (Fig. 1 b). This herpesvirus isolate was subsequently passaged, purified, and titered on primary rhesus fibroblasts, and vDNA was purified from cell-free virions for molecular characterization.

Table I. *Amino Acid Sequence Identity of RRV Strain 17577 Orfs with Orfs from Selected Herpesviruses or Human or Rhesus Macaque Cellular Homologues*

	Selected primate herpesviruses					Cellular homologues	
Orf	KSHV	HVS	RhEBV	RhCMV	RRV	Human	Rhesus
Pol	50.8	50.8	55.0	40.0	100	ND	NA
IL-6	12.7	NA	NA	NA	100	17.8	17.8
TS	66.1	64.6	NA	NA	NA	ND	NA
MIP	32.3 (MIP-II)	NA	NA	NA	NA	26.1 (MIP-1β)	NA

Amino acid sequences were aligned by GAP or CLUSTAL and the percent identity determined. Rh, rhesus; Pol, DNA polymerase; NA, not available.

The initial molecular characterization of the virus was conducted using degenerate PCR analysis targeting a conserved region of the vDNA polymerase gene (FDIEC-VYEFP) from beta- and gammaherpesviruses. Purified vDNA, which was capable of producing infectious virus from $CaCl_2$-transfected fibroblasts, was subjected to PCR, and the resulting fragments were cloned and sequenced. As controls, we included DNA from rhesus CMV– and rhesus EBV–infected cells as well as DNA from uninfected cells. This comparative analysis revealed that the virus was a gammaherpesvirus, as the deduced amino acid sequence was more closely related to rhesus EBV than rhesus CMV (Table I). Inclusion of amino acid sequences from other known gammaherpesviruses, such as KSHV and HVS, supported this assignment. Moreover, comparative analysis with the recently described RRV strain H26-95 revealed that the herpesvirus isolate recovered from rhesus macaque 17577 was an RRV.

To further characterize RRV strain 17577, we screened vDNA, restriction endonuclease digested with EcoRI, by Southern blot analysis for the presence of a TS gene, an unspliced cellular gene homologue that is conserved in KSHV and HVS but not EBV. Using a KSHV TS gene fragment as a probe, a single DNA fragment was found to hybridize under conditions of moderate stringency (data not shown). This DNA fragment was subsequently isolated and further digested for subcloning and DNA sequence determination.

DNA sequence analysis of a 3.4-kb fragment revealed three orfs, two with striking homology to KSHV and a single orf having 100% identity with RRV and limited homology to cellular IL-6 (Table I). One orf encodes a homologue of KSHV MIP-II with 30.9% amino acid sequence identity, as defined by the GAP program provided with the Wisconsin GCG analysis package, and the second

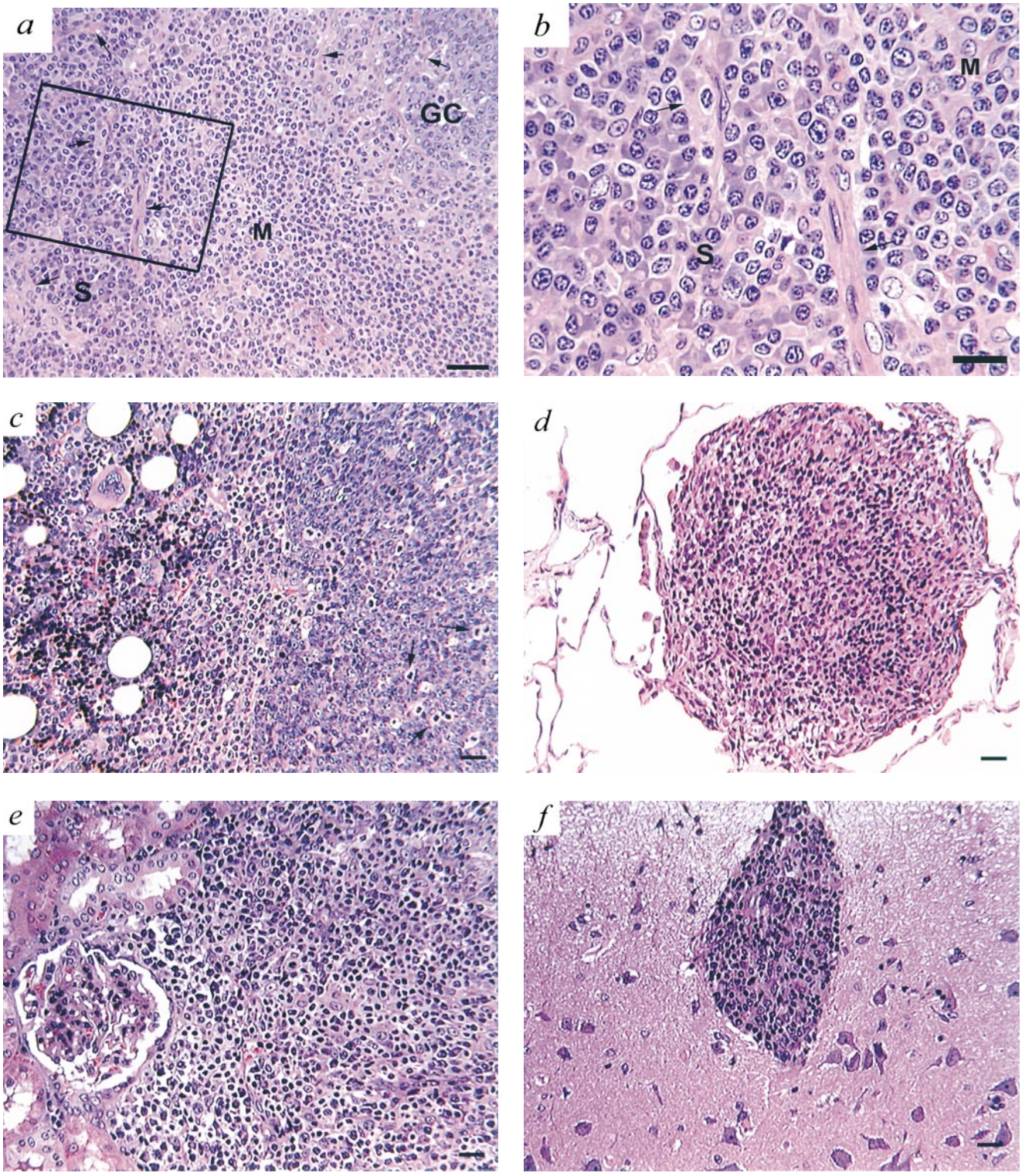

Figure 2. Multicentric lymphoproliferative disease in SIV_{mac}-infected rhesus macaque 17577. (a) Axillary LN with prominent, poorly defined, hyperplastic germinal centers (GC), rarified mantle zone (M), plasma cell infiltration in an accentuated interfollicular sinus (S), and stromovascular changes in the interfollicular zone and germinal center (arrows); bar, 40 μm. (b) Inset outlined in panel a illustrating marked plasmacytosis; bar, 20 μm. (c) Marked follicular lymphoid hyperplasia in BM with mitotic cells indicated by arrows. Multiple pleomorphic lymphoid nodules were present in lung (d), kidney (e), and brain (f).

orf encodes a homologue of both cellular and vTS, with 66 and 64.6% amino acid sequence identity with KSHV and HVS, respectively. The third orf revealed 100% identity with RRV strain H20-95 IL-6, supporting our initial finding that the 17577 virus is an RRV.

RRV Is Present in Tissue Harboring LPD. Rhesus macaque 17577 was humanely killed 503 d after SIV infection and found to have multicentric LPD involving both lymphoid and nonlymphoid tissues. Attempts to propagate continuously replicating or transformed cells from mononuclear cells dispersed from BM and LNs were unsuccessful. Histopathologically, there was marked follicular lymphoid hyperplasia in LNs, spleen, and BM. The follicular elements were dominated by giant, often irregularly shaped, secondary, reactive germinal centers. Follicular architecture in the cortices of LNs was accentuated by expanded cellular interfollicular zones dominated by plasma cells and vascular and stromal elements (Fig. 2, a and b). The medullary cords were densely populated by plasma cells, and arborizing cords of plasma cells extended into the paracortical zones. Follicular lymphoid hyperplasia was particularly striking in the BM (Fig. 2 c). The LPD lesions in nonlymphoid tissues were principally nodular, pleomorphic lymphoid masses composed of cytologically normal lymphocytes, plasma cells, and macrophage-like cells that effaced normal tissue architecture (Fig. 2, d and e).

To determine if the LPD lesions in macaque 17577 harbored RRV, oligonucleotide primers specific to the RRV MIP homologue were designed to detect vDNA by PCR amplification and Southern blot analysis. By semiquantitative PCR analysis, vDNA sequences were found to be present at >590 copies/0.1 μg of BM-derived DNA (Fig. 3 a). As most animals held in captivity are naturally infected with RRV (18, 36), BM aspirates were obtained from other animals to determine if RRV is a common resident of BM. BM samples were collected from two SIV-infected animals without peripheral lymphadenopathy, and two additional samples were obtained from animals that were killed due to disease unrelated to SIV infection or LPD. Analysis of these samples revealed no detectable signal, suggesting that RRV DNA in the BM-derived DNA from these four animals was either absent or below the limits of detection (Fig. 3 b). Finally, the BM-derived DNA from macaque 17577 was analyzed for rhesus EBV–specific sequences, as rhesus EBV has been shown to be associated with LPD in SIV-infected animals (37). No signal corresponding to rhesus EBV DNA sequences was detected (Fig. 3 c), indicating that rhesus EBV was not present in this lesion.

Experimental Inoculation of Macaques with RRV Strain 17577. To test whether RRV strain 17577 can cause disease in its natural host, six juvenile rhesus macaques were selected for experimental inoculation studies. All six macaques were ~1.5 yr old and shown to be negative for RRV infection over a 6-mo period by absence of RRV-specific serum antibody as measured by whole-virus ELISA, failure to detect RRV sequences in peripheral blood leukocytes by PCR analysis, and failure to isolate

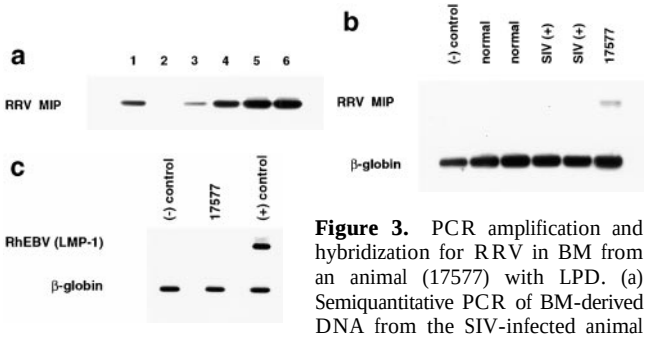

Figure 3. PCR amplification and hybridization for RRV in BM from an animal (17577) with LPD. (a) Semiquantitative PCR of BM-derived DNA from the SIV-infected animal with LPD for RRV MIP. Lane 1, BM-derived DNA; lane 2, 100 pg of DNA from uninfected cells; lane 3, 100 pg of DNA from uninfected cells plus 100 fg of vDNA; lane 4, 100 pg of DNA from uninfected cells plus 1 pg of vDNA; lane 5, 100 pg of DNA from uninfected cells plus 10 pg of vDNA; lane 6, 100 pg of DNA from uninfected cells plus 100 pg of vDNA. (b) PCR and Southern blot analysis of DNA amplified from BM for RRV MIP or rhesus β-globin gene. The source for each BM sample is indicated above each lane. The negative (−) control is DNA isolated from uninfected rhesus fibroblasts. (c) Southern blot analysis of DNA PCR amplified with oligonucleotide primers specific for the rhesus (Rh)EBV LMP-1 gene or rhesus β-globin gene. The source for each sample is indicated above each lane. The negative (−) control is DNA isolated from uninfected rhesus fibroblasts, and the positive (+) control is DNA from RhEBV-infected cells.

RRV from PBMCs cocultured with primary rhesus fibroblasts. As >75% of immunocompetent animals in our colony are seropositive for RRV by 3 yr of age and do not develop spontaneous LPD, we initially inoculated four of the animals with SIV_{mac239} to provide a background of immunosuppression before experimental RRV inoculation. 8 wk after SIV infection, two of the four animals inoculated with SIV (18483 and 18570) were inoculated intravenously with 5×10^6 PFU of cell-free RRV 17577. The two remaining SIV-infected animals (18503 and 18540) were maintained as SIV-only infection controls. Two additional animals (19092 and 19286) were infected with RRV 17577 to serve as RRV-only infection controls.

Sequential FACS™ analysis of PBMCs from the experimental animals revealed limited $CD4^+$ lymphocyte depletion (mean values = 900–1,100/μl) 2 wk after SIV infection in the SIV-infected animals, followed by a rebound and sustained $CD4^+$ lymphocyte counts in the normal range (mean values = 1,500–2,000/μl), whereas $CD8^+$ lymphocyte counts increased slightly compared with the preinoculation time points. Significant differences in the number of $CD20^+$ B lymphocytes were observed among the three groups of animals. As early as 6 wk after RRV infection, the number of $CD20^+$ B lymphocytes increased dramatically in the two RRV/SIV-infected macaques (mean values = 2,900–3,360/μl) and persisted for 34 wk in animal 18483 and 14 wk in animal 18570 (Fig. 4, a and b). In contrast, the SIV-infected control animals exhibited persistently low numbers of $CD20^+$ B lymphocytes (mean values = 200–300/μl) beginning 2 wk after SIV infection (Fig. 4, c and d). The number of circulating $CD20^+$ B lymphocytes increased slightly 2 wk after infection (mean values = 950–1,000/μl) in the RRV-only controls (Fig. 4, e

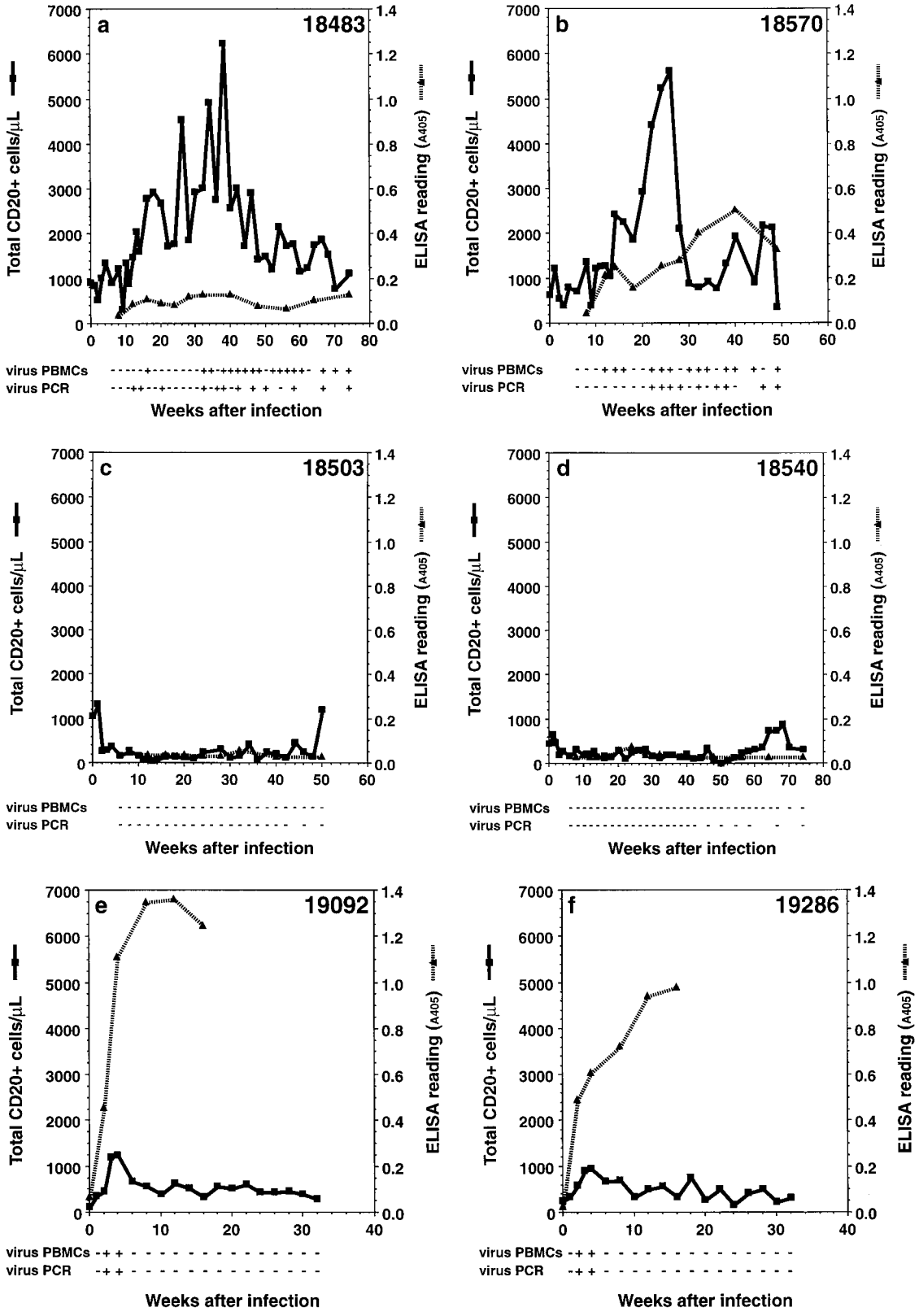

Figure 4. CD20$^+$ lymphocytes, antibody response, and RRV strain 17577 isolation/detection in SIV_{mac}-infected animals. Total CD20$^+$ cells were measured at the indicated weeks after infection, virus isolations (virus PBMCs) were determined by coculture of PBMCs with primary rhesus fibroblasts, and the presence of vDNA (virus PCR) was determined by PCR analysis on DNA derived from PBLs. Detection of antibodies to RRV strain 17577 were determined by ELISA on plates coated with extracts derived from RRV-infected cells. +, positive for virus culture or vDNA, as defined by PCR and Southern blot analysis; −, negative virus culture or vDNA. Animals 18483 (a) and 18570 (b) were experimentally inoculated with SIV_{mac239} and RRV strain 17577, animals 18503 (c) and 18540 (d) were experimentally inoculated with SIV_{mac239} only, and animals 19092 (e) and 19286 (f) were experimentally inoculated with RRV strain 17577.

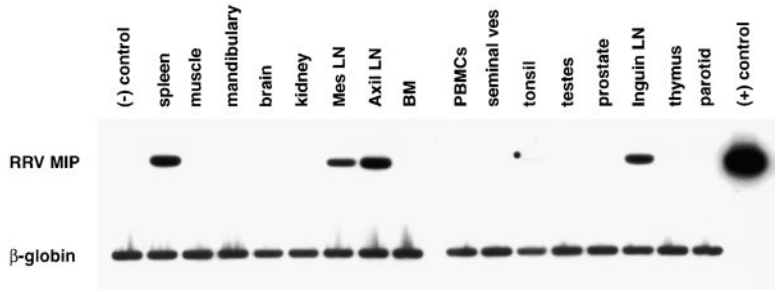

Figure 5. PCR analysis of PBLs and tissues from animal 18570 collected at necropsy for RRV DNA and rhesus β-globin. Mes, mesenteric; Axil, axillary; ves, vesicle; Inguin, inguinal; parotid, parotid gland.

and f). Further FACS™ analysis revealed that the PBMCs from the two RRV/SIV-infected macaques expressed the CD40 activation marker coincident with CD20 but not CD23, which is expressed after rhesus EBV infection (reference 38; data not shown).

RRV was readily recovered from PBMCs of the two RRV/SIV-infected animals as early as 4 wk after RRV infection in macaque 18570 and 8 wk after infection in macaque 18483. Subsequently, positive virus cultures were obtained repeatedly from these animals for the duration of the study (Fig. 4, a and b). The PBMCs from the two RRV/SIV-infected animals were also shown to harbor RRV DNA 4 wk after RRV inoculation in macaque 18483 and 14 wk after infection in macaque 18570, as determined by PCR and Southern blot analysis for the vMIP gene. Interestingly, no substantial difference in cell-associated viral load was discernible in PBMCs throughout the course of infection by PCR or virus isolation (data not shown). The two SIV-only control macaques were consistently negative for RRV by both methods of detection (Fig. 4, c and d). The RRV-only control macaques were positive for RRV by both methods of detection 2 wk after infection and remained positive through 6 wk after infection (Fig. 4, e and f).

The humoral response to RRV infection was assessed sequentially using a whole-virus ELISA. One of the two RRV/SIV-infected animals failed to develop a measurable antibody response to RRV, whereas a low antibody response to RRV was detected in the second RRV/SIV-infected macaque 4 wk after RRV infection (Fig. 4, a and b). Both of the SIV-only controls remained seronegative for RRV for the duration of the study (Fig. 4, c and d), whereas the two RRV-only controls developed strong sustained anti-RRV antibody responses beginning 2 wk after infection (Fig. 4, e and f).

Clinical and Pathological Findings. Early symptoms of SIV infection included fever, mild skin rash, and malaise, coincident with primary SIV p27 antigenemia in the four SIV-infected macaques by 2 wk after SIV infection. 10 wk after RRV infection, the two RRV/SIV-infected macaques developed marked peripheral lymphadenopathy, which persisted for >56 wk in macaque 18483 and 31 wk in macaque 18570. Additionally, the two RRV/SIV-infected macaques developed marked, persistent splenomegaly with spleens ~10 times normal size. 30 wk after RRV infection, macaque 18570 developed severe hemolytic anemia that was unresponsive to treatment with prednisolone and was killed 286 d after RRV infection. At necropsy, there was marked generalized lymphadenopathy, hepatomegaly, splenomegaly, diffuse erythroid hyperplasia in the BM, and membranous glomerulonephritis. Analysis of necropsy tissues for vDNA indicated that virus was present in all lymphoid organs (Fig. 5). Of particular interest is the absence of vDNA in the BM, which also did not exhibit lymphoid hyperplasia observed in the BM of macaque 17577 from which RRV 17577 was isolated. Only slight transient peripheral LN enlargement was seen in the SIV- and RRV-only control macaques, and splenomegaly was not observed.

Histopathologic examination of peripheral LN biopsy samples revealed marked differences between the three groups. 27 wk after RRV infection, LNs from the two RRV/SIV-infected macaques had marked angiofollicular lymphoid hyperplasia characterized by giant, secondary, reactive germinal centers that were frequently irregular in shape and lacked distinct mantle zones. Medullary cords and paracortical areas were infiltrated by sheets of plasma cells. The interfollicular zones were accentuated and relatively hypocellular, with increased vascularity and plasma cell infiltration (Fig. 6, a and b). The lymphoid hyperplasia was persistent and multicentric. Virtually all of the LNs recovered from macaque 18570 at necropsy were profoundly enlarged. The morphologic changes were similar to those observed in the LN biopsy 27 wk after RRV infection, with the exception that the necropsy LN samples contained a mix of both secondary reactive and tertiary regressive germinal centers, with vascular hyalinization in most LNs. Plasma cells dominated the medullary cords, paracortex, and interfollicular zones. The spleen of macaque 18570 also contained large, irregularly shaped lymphoid follicles that lacked mantles and were composed of a mosaic pattern of hyalinized cell-poor areas and cellular areas of normally proliferating germinal center lymphocytes. Cords and islands of mature plasma cells were prevalent in the red pulp (data not shown). In contrast, LNs from the control SIV animals, collected 35 wk after SIV infection, had profoundly atrophied lymphoid follicles and hypocellular paracortices with condensed stromal elements characteristic of SIV-induced lymphoid atrophy (Fig. 6 c; reference 39). LN biopsies from the two RRV control macaques 9 wk after infection had normal histologic features (Fig. 6 d).

Immunophenotyping of LN mononuclear cells revealed significant differences in the number of $CD20^+$ B lym-

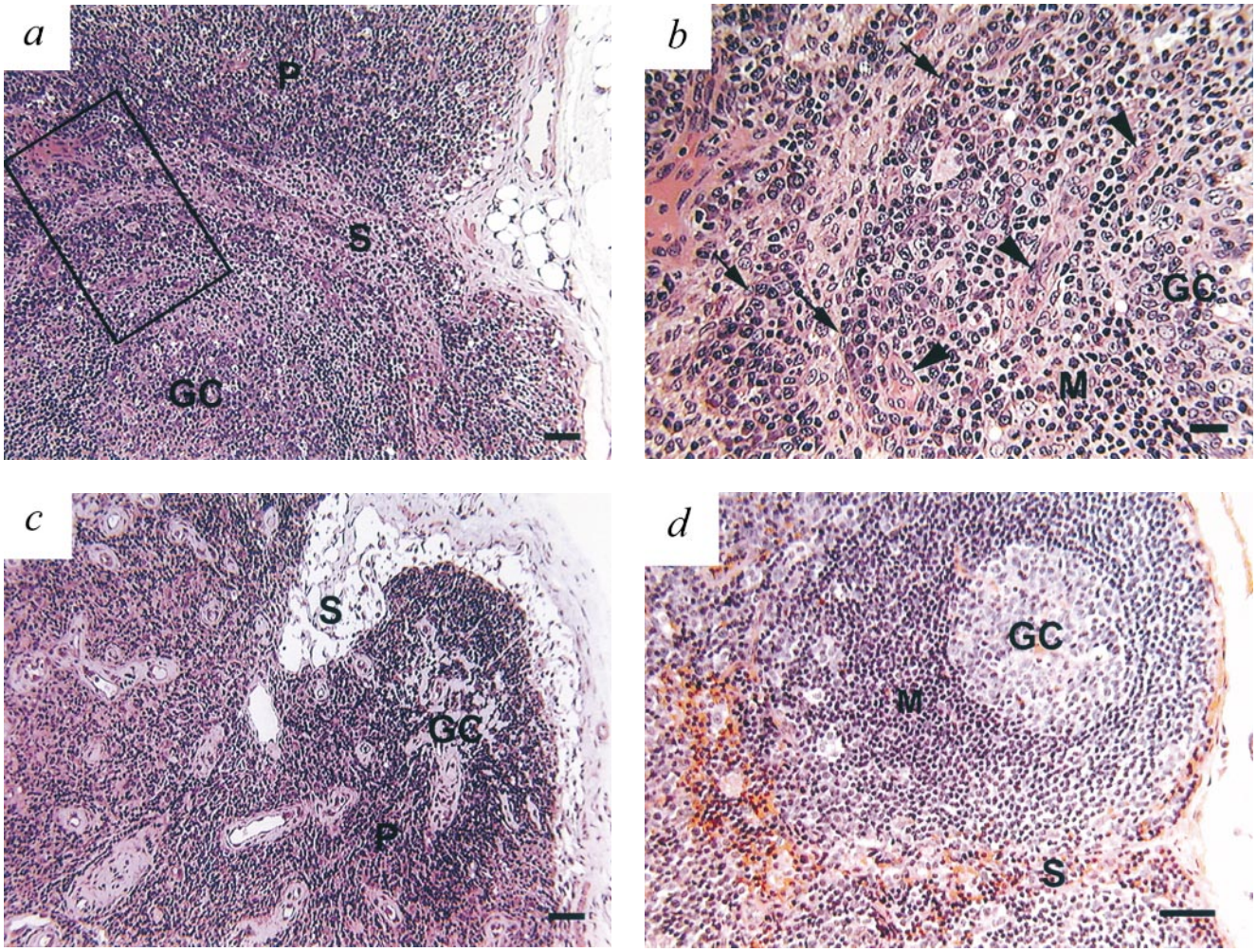

Figure 6. Axillary LNs from RRV/SIV-, SIV-, and RRV-infected animals. (a) Angiofollicular lymphoid hyperplasia in SIV_{mac}- and RRV-infected macaque 18570 with prominent germinal center (GC) and cellular interfollicular sinus (S) and paracortex (P). (b) Higher magnification of boxed area in panel a, with numerous interfollicular plasma cells (arrows), increased vascular stroma with hypertrophied endothelial cells (arrow heads), and effaced mantle zone (M). (c) Marked lymphoid atrophy in SIV_{mac}-only control macaque 18503. The cortex is thin and sinuses (S) are dilated. Involuted, hyalinized germinal centers (GC) are difficult to visualize, and the paracortex (P) consists of condensed stroma and sparse small lymphocytes. (d) Normal follicular architecture in RRV-only control macaque 19286. Hematoxylin and Lee stain; bars: a, 50 μm; b, 25 μm; c, 50 μm; and d, 50 μm.

phocytes in the LNs from the two RRV/SIV-infected macaques compared with LNs from macaques in the SIV- and RRV-only control groups. The four animals in the two control groups had twofold increases in the number of LN $CD20^+$ B lymphocytes compared with preinoculation samples, whereas the two RRV/SIV-infected animals had fourfold increases in the number of $CD20^+$ B lymphocytes compared with the preinoculation control samples and twofold increases over the postinfection samples from the two control groups (Fig. 7). Attempts to culture continuously replicating or transformed cells from dispersed LN mononuclear cells and PBMCs were unsuccessful.

Coinfection with SIV and RRV resulted in a marked increase in serum IgG (Table II). Two RRV/SIV experimentally infected macaques, as well as macaque 17577 from which RRV strain 17577 was recovered, developed marked hypergammaglobulinemia (serum IgG >2,000 mg/dl). κ and λ Light chain levels in total plasma Ig increased from mean preinfection values of 96 and 121 mg/dl in 17577 and the two RRV/SIV experimentally infected macaques to 149 and 212 mg/dl, respectively. The pre- and postinfection mean κ and λ light chain ratios were 0.8 and 0.7, respectively, indicating that the increase in plasma light chain concentrations was not associated with appreciable skewing. Postinfection total plasma Ig κ and λ levels decreased in the single SIV-only animal tested (18503), also without appreciable skewing. Terminal serum from macaque 18570 was also positive in the direct antiglobulin (Coombs') test, strongly suggesting that the hemolytic anemia in this animal was immune mediated. Modestly elevated serum IgG (1,233 mg/dl) was noted in SIV-only control macaque 18540. Increases in serum IgG were not observed in the second SIV-only control macaque or the two RRV-only control macaques (serum IgG <700 mg/dl).

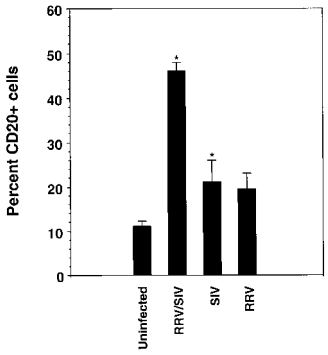

Figure 7. Histogram of percent $CD20^+$ cells detectable in dissociated LNs of uninfected controls and RRV/SIV-infected, SIV-infected, and RRV-infected animals. Data are mean ± SEM; $*P < 0.05$ compared with uninfected controls.

Normal polyclonal electrophoretic profiles were obtained from all serum samples (data not shown).

Table II. *Concentration of Plasma Gammaglobulin in SIV and/or RRV Experimentally Inoculated Rhesus Macaques*

Animal no.	Before inoculation	Weeks after SIV inoculation					
		16	30	42	50	70	84
17577*	784	NA	NA	NA	NA	2,448¶	
18483‡	621	1,243	2,096	NA	2,490	NA	5,055
18570‡	811	1,507	3,004	NA	1,795¶**		
18503§	661	585	536	NA	211¶		
18540§	789§	607	743	NA	871	NA	1,233
19092‖	494	NA	NA	564			
19286‖	742	NA	NA	648			

IgG concentrations (mg/dl) were determined at different weeks after SIV inoculation by nephelometry.
*Animal 17577 was the SIV-infected macaque with LPD and the source of RRV strain 17577.
‡Animals experimentally inoculated with RRV and SIV.
§Animals experimentally inoculated with SIV only.
‖Animals experimentally inoculated with RRV only.
¶Samples obtained at necropsy.
**Treated with prednisolone for hemolytic anemia at 2 mg/kg beginning 42 wk after SIV inoculation.
NA, samples not analyzed.

Discussion

In this study, we describe the isolation of RRV strain 17577 from an SIV-infected rhesus macaque that eventually developed LPD. Like the RRV isolate previously described by Desrosiers et al. (18), strain H26-95, the isolate described here encodes a vIL-6–like cytokine gene. Moreover, this isolate also contains a vMIP-like homologue with amino acid sequence identity to KSHV vMIP-II. Sequence analysis of the entire RRV strain 17577 genome has recently been completed and reveals that the genome is essentially colinear with KSHV and possesses similar genes with the potential for transformation, regulation of apoptosis, or growth control as KSHV (40). In particular, RRV possesses a gene, referred to as R1, in the same position as saimiri transforming protein and K1 of HVS and KSHV, respectively. BLAST analysis with R1 shows that the NH_2 terminus is similar to that of the Fc receptor, suggesting that R1 is a transmembrane receptor and therefore may be involved in signal transduction and transformation. RRV stain 17577 is also >99% identical at the DNA level to the regions of the RRV strain H26-95 genome available for analysis. The majority of base differences are found in the midregion of orf 8, glycoprotein B, and predicted to encode both conserved and nonconserved changes in the protein. Geographical variation in KSHV is increasingly documented in association with different forms of KS and KSHV infection rates and raises the possibility that sequence variation may relate to differences in virulence or transmission (41–45). Interestingly, genotypic differences in glycoprotein B of human CMV are postulated to be associated with increased virulence in BM transplant recipients (46). This same region has not been analyzed from different isolates of KSHV derived from AIDS-related KS, classical/endemic KS, or LPD, and the significance of the sequence variation in the RRV glycoprotein B gene is unknown.

RRV strain 17577 was recovered from the BM of a naturally infected rhesus macaque that developed profound, persistent angiofollicular peripheral lymphadenopathy after experimental infection with a macrophage-tropic variant of SIV_{mac239}. Subclinical multicentric involvement of lymphoid tissues and solid organs was found at necropsy 503 d after SIV infection. PCR analysis of BM tissue exhibiting lymphocytic hyperplasia revealed that RRV DNA was present in high copy number but not in BM from normal macaques or in macaque 18570. We speculate that the difference in viral load in the BM of animal 18570 may be due to the lack of LPD in the BM, compared with the florid LPD lesions observed in the BM of macaque 17577.

As a causal role for RRV in the development of these lesions cannot be established by PCR analysis alone, we undertook experimental inoculation studies in rhesus macaques to determine whether RRV is just a ubiquitous agent in nonhuman primates or a pathogen capable of inducing disease manifestations in its natural host. The absence of B cell hyperplasia in the SIV- or RRV-only controls and the presence of high RRV loads in hyperplastic lymphoid tissues from SIV and RRV–coinfected macaques indicate that B cell hyperplasia is strongly associated with RRV. A role for RRV in B cell hyperplasia or LPDs is consistent with the biology of most or all other gammaherpesviruses (KSHV, EBV, MHV-68, HVS). The index macaque and the macaques experimentally infected with SIV_{mac239} and RRV 17577 developed profound, persistent, multicentric angiofollicular lymphadenopathy resembling the multicentric plasma cell form of MCD either in the absence or presence of HIV infection (47). The hypergammaglobulinemia in the index macaque and both experimental RRV/SIV-infected macaques and the fatal immune-mediated hemolytic anemia in one of the two experimentally RRV/SIV-infected macaques are also clinical features that

closely parallel those observed in KSHV-infected AIDS patients and HIV-1–seronegative patients with MCD (48–50).

Both SIV and HIV-1 induce in vivo B lymphocyte hyperactivation, as shown by hypergammaglobulinemia, circulating immune complexes, and sometimes elevated levels of autoantibodies (49, 51, 52). However, the consort of profound hypergammaglobulinemia, immune-mediated hemolytic anemia, and progressive lymphadenopathy reported here are unusual disease manifestations in SIV_{mac}-infected macaques, and few cases are reported (20, 39, 53, 54). The RRV infection status in these animals is not known, as RRV was only recently identified. The absence of hypergammaglobulinemia, immune-mediated hemolytic anemia, and persistent angiofollicular lymphadenopathy in our SIV_{mac239}-only and RRV-only infection control macaques suggest that RRV coinfection may be an important factor in the immunopathogenesis of retrovirus-induced immunodeficiency disease in macaques. This cofactor role has long been recognized for EBV in human AIDS patients, and a similar role is evolving for KSHV.

Despite the significant evidence of B cell hyperplasia in the peripheral blood, LNs, and spleens of the RRV/SIV coinfected animals, they do not appear to have overt clonal abnormalities in their B cells, nor were we able to establish continuously replicating primary B lymphocyte cultures from them. This differs considerably from rhesus EBV infection, where we have been able to generate continuously replicating cultures of rhesus EBV–positive B cells in vitro from PBMCs collected from naturally infected macaques (our unpublished results). The evolution of clonal abnormalities in LPDs is complex (55), and although monoclonality was not evident in the LPD manifested in the RRV/SIV-coinfected animals, minor clonal abnormalities may be present. Recent studies suggest that differential expression of rhadinovirus cytokine and oncogene homologues may play an important role in the development of B cell hyperplasia and other abnormal cellular proliferations (15, 48, 56, 57). Although one of the experimental RRV/SIV-infected macaques developed fatal immune-mediated hemolytic anemia, none of the macaques developed lymphoma, and continuously replicating lymphoid cells could not be obtained from the RRV-positive, hyperplastic lymphoid tissues or peripheral blood. Immortalized $KSHV^+$ cell lines have also not been established from healthy $KSHV^+$ carriers or KS and MCD patients, with the exception of a continuously replicating $KSHV^+/EBV^-$ cell line obtained from the peripheral blood of an HIV-seronegative patient with PEL who exhibited a phenotype similar to PEL-derived cell lines (58). Thus, like KSHV, RRV may require other transforming events or cofactors for lymphomas to develop.

Consistent with the association between high RRV load and B lymphocyte hyperplasia reported here, we have recently shown that healthy RRV carrier macaques harbor RRV in their $CD20^+$ B lymphocytes in vivo (59). Recent studies support the hypothesis that KSHV vIL-6 plays an important role in the pathogenesis of PEL and MCD (48, 57), and a similar role for the RRV IL-6–like cytokine is under investigation. Preliminary analysis of the RRV IL-6–like cytokine reveals that it can functionally substitute for cellular IL-6 in IL-6 bioassays (60). IL-6 is a cytokine with several functions, including the ability to activate B cells into immunoglobulin-producing cells. More importantly, IL-6 dysregulation appears to be a factor in the development of MCD and multiple myeloma (61, 62).

The experimental infection protocol used here, SIV_{mac239} infection before RRV infection, was designed to provide RRV a replicative advantage, as most herpesviruses, e.g., CMV and EBV, manifest disease in immunocompromised hosts. Moreover, serological analysis of the animals at ORPRC and other primate facilities reveal that >90% of immunocompetent animals are seropositive for RRV. Despite the high prevalence rates, few animals develop LPD, implying that the host immune response is capable of controlling the virus infection. What role SIV_{mac239} infection plays in the disease manifestations reported here is not clear. One possible mechanism is that SIV-induced immunosuppression may be important for sustained RRV infection and replication. Some have proposed a similar cofactor role for HIV-1 in AIDS-related KS and PEL, whereas others believe, at least in the histogenesis of KS, that HIV-1 invokes an inflammatory response, promoting an increase in inflammatory cytokines that sustain KS lesions (15). We believe that RRV is likely an opportunistic infection in the SIV-infected animals, given the absence of similar disease manifestations in animals experimentally inoculated with RRV or SIV alone.

Finally, in addition to providing an animal model for some aspects of KSHV pathogenesis, coinfection studies such as those described here should be important for AIDS pathogenesis. Preliminary results suggest that the presence of RRV attenuates SIV replication. The KSHV MIP-II protein has been shown to inhibit CCR-dependent HIV infection in vitro (63, 64). Like HIV, genetically divergent strains of SIV utilize CCR5 and other orphan seven-transmembrane receptors for viral entry (65–69). With the availability of manipulatable molecular clones, we expect that RRV will be extremely useful as an animal model for studying aspects of both KSHV and AIDS pathogenesis. One significant advantage of RRV is that it can be propagated and plaque titered in cultured cells, allowing molecular dissection of genes postulated to be related to pathogenesis. Studies are in progress to determine the role of the vIL-6 homologue and other viral genes in KSHV-induced disease and in this animal model of B cell hyperplasia.

We thank Drs. Ann B. Hill, David Johnson, Jay Nelson, and Robert P. Searles for helpful discussions and Ms. Lori Boshears for assistance with the manuscript.

This work was supported by Public Health Service grants RR00163 and CA75922.

Address correspondence to Scott W. Wong, Division of Pathobiology and Immunology, Oregon Regional Primate Research Center, 505 NW 185th Ave., Beaverton, OR 97006. Phone: 503-690-5285; Fax: 503-690-5524; E-mail: wongs@ohsu.edu

Submitted: November 1998 Revised: 13 July 1999 Accepted: 14 July 1999

References

1. Beral, V., T.A. Peterman, R.L. Berkelman, and H.W. Jaffe. 1990. Kaposi's sarcoma among persons with AIDS: a sexually transmitted infection? *Lancet*. 335:123–128.
2. Chang, Y., E. Cesarman, M.S. Pessin, F. Lee, J. Culpepper, D.M. Knowles, and P.S. Moore. 1994. Identification of herpesvirus-like DNA sequences in AIDS-associated Kaposi's sarcoma. *Science*. 266:1865–1869.
3. Schalling, M., M. Ekman, E.E. Kaaya, A. Linde, and P. Biberfeld. 1995. A role for a new herpes virus (KSHV) in different forms of Kaposi's sarcoma. *Nat. Med*. 1:707–708.
4. Moore, P.S., and Y. Chang. 1995. Detection of herpesvirus-like DNA sequences in Kaposi's sarcoma in patients with and those without HIV infection. *N. Engl. J. Med*. 332:1181–1185.
5. Huang, Y.Q., J.J. Li, M.H. Kaplan, B. Poiesz, E. Katabira, W.C. Zhang, D. Feiner, and A.E. Friedman-Kien. 1995. Human herpesvirus-like nucleic acid in various forms of Kaposi's sarcoma. *Lancet*. 345:759–762.
6. Whitby, D., M.R. Howard, M. Tenant-Flowers, N.S. Brink, A. Copas, C. Boshoff, T. Hatzioannou, F.E. Suggett, D.M. Aldam, A.S. Denton, et al. 1995. Detection of Kaposi sarcoma-associated herpesvirus in peripheral blood of HIV-infected individuals and progression to Kaposi's sarcoma. *Lancet*. 346:799–802.
7. Ambroziak, J.A., D.J. Blackbourn, B.G. Herndier, R.G. Glogau, J.A. Gullett, A.R. McDonald, E.T. Lennette, and J.A. Levy. 1995. Herpes-like sequences in HIV-infected and uninfected Kaposi's sarcoma patients. *Science*. 268:582–583.
8. Dupin, N., M. Grandadam, V. Calvez, I. Gorin, J.T. Aubin, S. Havard, F. Lamy, M. Leibowitch, J.M. Huraux, J.P. Escande, et al. 1995. Herpesvirus-like DNA in patients with Mediterranean Kaposi's sarcoma. *Lancet*. 345:761–762.
9. Chuck, S., R.M. Grant, E. Katongole-Mbidde, M. Conant, and D. Ganem. 1996. Frequent presence of a novel herpesvirus genome in lesions of human immunodeficiency virus-negative Kaposi's sarcoma. *J. Infect. Dis*. 173:248–251.
10. O'Neill, E., T.H. Henson, A.J. Ghorbani, M.A. Land, B.L. Webber, and J.V. Garcia. 1996. Herpesvirus-like sequences are specifically found in Kaposi sarcoma lesions. *J. Clin. Pathol*. 49:306–308.
11. Cesarman, E., Y. Chang, P.S. Moore, J.W. Said, and D.M. Knowles. 1995. Kaposi's sarcoma-associated herpesvirus-like DNA sequences in AIDS-related body-cavity-based lymphomas. *N. Engl. J. Med*. 332:1186–1191.
12. Nador, R.G., E. Cesarman, A. Chadburn, D.B. Dawson, M.Q. Ansari, J. Sald, and D.M. Knowles. 1996. Primary effusion lymphoma: a distinct clinicopathologic entity associated with the Kaposi's sarcoma-associated herpesvirus. *Blood*. 88:645–656.
13. Otsuki, T., S. Kumar, B. Ensoli, D.W. Kingman, T. Yano, M. Stetler-Stevenson, E.S. Jaffe, and M. Raffeld. 1996. Detection of HHV-8/KSHV DNA sequences in AIDS-associated extranodal lymphoid malignancies. *Leukemia*. 10:1358–1362.
14. Soulier, J., L. Grollet, E. Oksenhendler, P. Cacoub, D. Cazals-Hatems, P. Babinet, M.F. d'Agay, J.P. Clauvel, M. Raphael, L. Degos, et al. 1995. Kaposi's sarcoma-associated herpesvirus-like DNA sequences in multicentric Castleman's disease. *Blood*. 86:1276–1280.
15. Gallo, R.C. 1998. Some aspects of the pathogenesis of HIV-1 associated Kaposi's sarcoma. *J. Natl. Cancer Inst. Monogr*. 23: 55–57.
16. Moore, P.S., C. Boshoff, R.A. Weiss, and Y. Chang. 1996. Molecular mimicry of human cytokine and cytokine response pathway genes by KSHV. *Science*. 274:1739–1744.
17. Nicholas, J., V.R. Ruvolo, W.H. Burns, G. Sandford, X. Wan, D. Ciufo, S.B. Hendrickson, H.-G. Guo, G.S. Hayward, and M.S. Reitz. 1997. Kaposi's sarcoma-associated human herpesvirus-8 encodes homologues of macrophage inflammatory protein-1 and interleukin-6. *Nat. Med*. 3:287–292.
18. Desrosiers, R.C., V.G. Sasseville, S.C. Czajak, X. Zhang, K.G. Mansfield, A. Kaur, R.P. Johnson, A.A. Lackner, and J.U. Jung. 1997. A herpesvirus of rhesus monkeys related to the human Kaposi's sarcoma-associated herpesvirus. *J. Virol*. 71:9764–9769.
19. Baskin, G.B., L.N. Martin, S.R.S. Rangan, B.J. Gormus, M. Murphey-Corb, R.H. Wolf, and K.F. Soike. 1986. Transmissable lymphoma and simian acquired immunodeficiency syndrome in rhesus monkeys. *J. Natl. Cancer Inst*. 77:127–139.
20. Chalifoux, L.V., N.L. King, M. Daniel, M. Kannagi, R.C. Desrosiers, P.K. Sehgal, L.M. Waldron, R.D. Hunt, and N.L. Letvin. 1986. Lymphoproliferative syndrome in an immunodeficient rhesus monkey naturally infected with an HTLV-III-like virus (STLV-III). *Lab. Invest*. 55:43–50.
21. Tsai, C.C., C.C. Tsai, S.T. Roodman, and M.D. Woon. 1990. Mesenchymoproliferative disorders (MPD) in simian AIDS associated with SRV-2 infection. *J. Med. Primatol*. 19: 189–202.
22. Feichtinger, H., P. Putkonen, C. Parravicini, S.L. Li, E. Kaaya, D. Böttiger, G. Biberfeld, and P. Biberfeld. 1990. Malignant lymphomas in cynomolgus monkeys infected with simian immunodeficiency virus. *Am. J. Pathol*. 137:1311–1315.
23. Rose, T.M., K.B. Strand, E.R. Schultz, G. Schaefer, G.W. Rankin, Jr., M.E. Thouless, C.C. Tsai, and M.L. Bosch. 1997. Identification of two homologs of the Kaposi's sarcoma-associated herpesvirus (human herpesvirus 8) in retroperitoneal fibromatosis of different macaque species. *J. Virol*. 71:4138–4144.
24. Swanson, R., E. Bergquam, and S.W. Wong. 1998. Characterization of rhesus cytomegalovirus genes associated with anti-viral susceptibility. *Virology*. 240:338–348.
25. Rangan, S.R.S., L. Martin, N. Wang, and B.J. Gormus. 1986. Epstein-Barr virus-related herpesvirus from a Rhesus monkey (*Macaca mulatta*) with malignant lymphoma. *Int. J. Cancer*. 38:425–432.

26. Higgins, D.G., and P.M. Sharp. 1989. Fast and sensitive multiple sequence alignments on a microcomputer. *Comput. Appl. Biosci*. 5:151–153.
27. Renne, R., W. Zhong, B. Herndier, M. McGrath, N. Abbey, D. Kedes, and D. Ganem. 1996. Lytic growth of Kaposi's sarcoma-associated herpesvirus (human herpesvirus 8) in culture. *Nat. Med*. 2:342–346.
28. Russo, J.J., R.A. Bohenzhy, M.-C. Chein, J. Chen, M. Yan, D. Maddalena, J.P. Parry, D. Peruzzi, I.S. Edelman, Y. Chang, et al. 1996. Nucleotide sequence of the Kaposi's sarcoma-associated herpesvirus (HHV8). *Proc. Natl. Acad. Sci. USA*. 93:14862–14867.
29. Franken, M., O. Devergne, M. Rosenzweig, B. Annis, E. Kieff, and F. Wang. 1996. Comparative analysis identifies conserved tumor necrosis factor receptor-associated factor 3 binding sites in the human and simian Epstein-Barr virus oncogene LMP-1. *J. Virol*. 70:7819–7826.
30. Savatier, P., G. Trabuchet, Y. Chebloune, C. Faure, G. Verdier, and V.M. Nigon. 1987. Nucleotide sequence of the beta-globin genes in gorilla and macaque: the origin of nucleotide polymorphisms in humans. *J. Mol. Evol*. 24:309–318.
31. Kodama, T., D.P. Silva, M.D. Daniel, J.E. Phillips-Conroy, C.J. Jolly, J. Rogers, and R.C. Desrosiers. 1989. Prevalence of antibodies to SIV in baboons in their natural habitat. *AIDS Res. Hum. Retroviruses.* 5:337–343.
32. Endres, C.L., E. Bergquam, M.K. Axthelm, and S.W. Wong. 1995. Assessing genetic-based therapies for AIDS using the simian immunodeficiency virus. *J. Med. Primatol.* 24:141–144.
33. Naidu, Y.M., H.W. Kestler, Y. Li, C.V. Butler, D.P. Silva, D.K. Schmidt, C.D. Troup, P.K. Sehgal, P. Sonigo, M.D. Daniel, et al. 1988. Characterization of infectious molecular clones of simian immunodeficiency virus (SIVmac) and human immunodeficiency virus type 2: persistent infection of rhesus monkeys with molecularly cloned SIVmac. *J. Virol*. 62:4691–4696.
34. Kinter, C., and B. Sugden. 1981. Identification of antigenic determinants unique to the surfaces of cells transformed by Epstein-Barr virus. *Nature*. 294:458–460.
35. Clark, E.A., and J.A. Ledbetter. 1986. Activation of human B cells mediated through two distinct cell surface differentiation antigens, Bp35 and Bp50. *Proc. Natl. Acad. Sci. USA*. 83: 4494–4498.
36. Desrosiers, R.C. 1997. The value of specific pathogen-free rhesus monkey breeding colonies for AIDS research. *AIDS Res. Hum. Retroviruses.* 13:5–6.
37. Feichtinger, H., S.L. Li, E. Kaaya, P. Putkonen, K. Grunewald, K. Weyrer, D. Bottiger, I. Ernberg, A. Linde, G. Biberfeld, et al. 1993. A monkey model for Epstein-Barr virus–associated lymphomagenesis in human acquired immunodeficiency syndrome. *J. Exp. Med*. 176:281–286.
38. Moghaddam, A., M. Rosenzweig, D. Lee-Parritz, B. Annis, R.P. Johnson, and F. Wang. 1997. An animal model for acute and persistent Epstein-Barr virus infection. *Science*. 276: 2020–2033.
39. Chalifoux, L.V., D.J. Ringler, N.W. King, P.K. Sehgal, R.C. Desrosiers, M.D. Daniel, and N.L. Letvin. 1987. Lymphadenopathy in macaques experimentally infected with the simian immunodeficiency virus (SIV). *Am. J. Pathol*. 128: 104–110.
40. Searles, R.P., E.P. Bergquam, M.K. Axthelm, and S.W. Wong. 1999. Sequence and genomic analysis of a rhesus macaque rhadinovirus with similarity to Kaposi's sarcoma-associated herpesvirus/human herpesvirus 8. *J. Virol*. 73: 3040–3053.
41. Zong, J.-C., C. Metroka, M.S. Reitz, J. Nicholas, and G.S. Hayward. 1997. Strain variability among Kaposi sarcoma-associated herpesvirus (human herpesvirus 8) genomes: evidence that a large cohort of United States AIDS patients may have been infected by a single common isolate. *J. Virol*. 71: 2505–2511.
42. Luppi, M., P. Barozzi, R. Marasca, M.G. Ferrari, and G. Torelli. 1997. Human herpesvirus 8 strain variability in clinical conditions other than Kaposi's sarcoma. *J. Virol*. 71:8082–8083.
43. DiAlberti, L., S.L. Ngui, S.R. Porter, P.M. Speight, C.M. Scully, J.M. Zakrewska, I.G. Williams, L. Artese, A. Piattelli, and C.G. Teo. 1997. Presence of human herpesvirus 8 variants in the oral tissues of human immunodeficiency virus-infected persons. *J. Infect. Dis*. 175:703–707.
44. Foreman, K.E., S. Alkan, A.E. Krueger, J.R. Panella, L.J. Swinnen, and B.J. Nickoloff. 1998. Geographically distinct HHV-8 DNA sequences in Saudi Arabian iatrogenic Kaposi's sarcoma lesions. *Am. J. Pathol*. 153:1001–1004.
45. Kasolo, F.C., M. Monze, N. Obel, R.A. Anderson, C. French, and U.A. Gompels. 1998. Sequence analyses of human herpesvirus-8 strains from both African human immunodeficiency virus-negative and -positive childhood endemic Kaposi's sarcoma show a close relationship with strains identified in febrile children and high variation in the K1 glycoprotein. *J. Gen. Virol*. 79:3055–3065.
46. Fries, B.C., S. Chou, M. Boeckh, and B. Torok-Storb. 1994. Frequency distribution of cytomegalovirus envelope glycoprotein genotypes in bone marrow transplant recipients. *J. Infect. Dis*. 169:769–774.
47. Frizzera, G., B.A. Peterson, E.D. Bayrd, and A.A. Goldman. 1985. A systemic lymphoproliferative disorder with morphologic features of Castleman's disease: clinical findings and clinicopathologic correlations in 15 patients. *J. Clin. Oncol*. 3:1202–1216.
48. Parravicini, C., M. Corbellino, M. Paulli, U. Magrini, M. Lazzarino, P.S. Moore, and Y. Chang. 1997. Expression of a virus-derived cytokine, KSHV vIL-6 in HIV-seronegative Castleman's disease. *Am. J. Pathol.* 151:1517–1522.
49. Lane, H.C., H. Masur, L.C. Edgar, G. Whalen, A.H. Rook, and A.S. Fauci. 1983. Abnormalities of B-cell activation and immunoregulation in patients with the acquired immunodeficiency syndrome. *N. Engl. J. Med*. 309:453–458.
50. Martinez-Maza, O., E. Crabb, R.T. Mitsuyasu, J.L. Fahey, and J.V. Giorgi. 1987. Infection with the human immunodeficiency virus (HIV) is associated with an in vivo increase in B lymphocyte activation and immaturity. *J. Immunol*. 138: 3720–3724.
51. Schnittman, S.M., C.H. Lone, S. Higgins, T. Folks, and A.S. Fauci. 1986. Direct polyclonal activation of human B lymphocytes by acquired immunodeficiency virus. *Science*. 233: 1084–1086.
52. Rosenberg, Y.J., M.G. Lewis, and M.H. Kosco-Vilbois. 1998. Enhanced follicular dendritic cell-B cell interaction in HIV and SIV infections and its potential role in polyclonal cell activation. *Dev. Immunol*. 6:61–70.
53. Klumpp, S.A., F.J. Novembre, D.C. Anderson, M.A. Simon, D.J. Ringler, and H.M. McClure. 1993. Clinical and pathologic findings in infant rhesus macaques infected with SIVsmm by maternal transmission. *J. Med. Primatol.* 22:169–173.
54. Baba, T.W., Y.S. Jeong, D. Penninck, R. Bronson, M.F. Greene, and R.M. Ruprecht. 1995. Pathogenicity of live, at-

tenuated SIV after mucosal infection of neonatal macaques. *Science*. 267:1820–1825.
55. Knowles, D.M. 1999. Immunodeficiency-associated lymphoproliferative disorders. *Mod. Pathol*. 12:200–217.
56. Teruya-Feldstein, J., P. Zauber, J.E. Setsuda, E.L. Berman, L. Sorbara, M. Raffeld, G. Tosato, and E.S. Jaffe. 1998. Expression of human herpesvirus-8 oncogene and cytokine homologs in an HIV-seronegative patient with multicentric Castleman's disease and primary effusion lymphoma. *Lab. Invest*. 78:1637–1642.
57. Staskus, K.A., R. Sun, G. Miller, P. Racz, A. Jaslowski, C. Metroka, H. Brett-Smith, and A.T. Hasse. 1999. Cellular tropism and viral interleukin-6 expression distinguish human herpesvirus 8 involvement in Kaposi's sarcoma, primary effusion lymphoma, and multicentric Castleman's disease. *J. Virol*. 73:4181–4187.
58. Boschoff, C., S.J. Gao, L.E. Healy, S. Matthews, A.J. Thomas, L. Coignet, R.A. Warnke, J.A. Strauchen, E. Matutes, O.W. Kamel, et al. 1998. Establishing a $KSHV^+$ cell line (BCP-1) from peripheral blood and characterizing its growth in Nod/SCID mice. *Blood*. 91:1671–1679.
59. Bergquam, E.P., N. Avery, S.M. Shiigi, M.K. Axthelm, and S.W. Wong. 1999. Rhesus rhadinovirus establishes a latent infection in B lymphocytes in vivo. *J. Virol*. 73:7874–7876.
60. Kaleeba, J.A.R., E.P. Bergquam, and S.W. Wong. 1999. A rhesus macaque rhadinovirus related to Kaposi's sarcoma-associated herpesvirus/human herpesvirus 8 encodes a functional homologue of interleukin-6. *J. Virol*. 73:6177–6181.
61. Yoshizaki, K., T. Matsuda, N. Nishimoto, T. Kuritani, L. Taeho, K. Aozasa, T. Nakahata, H. Kawai, H. Tagoh, T. Komori, et al. 1989. Pathogenic significance of interleukin-6 (IL-6/BSF-2) in Castleman's disease. *Blood*. 74:1360–1367.
62. Kishimoto, T., S. Akira, and T. Taga. 1992. Interleukin-6 and its receptor: a paradigm for cytokines. *Science*. 258:593–597.
63. Kledal, T.N., M.M. Rosenkilde, F. Coulin, G. Simmons, A.H. Johnsen, S. Alouani, C.A. Power, H.R. Luttichau, J. Gerstoft, P.R. Clapham, et al. 1997. A broad-spectrum chemokine antagonist encoded by Kaposi's sarcoma-associated herpesvirus. *Science*. 277:1656–1659.
64. Boshoff, C., Y. Endo, P.D. Collins, Y. Takeuchi, J.D. Reeves, V.L. Schweickart, M.A. Siani, T. Sasaki, T.J. Williams, P.W. Gray, et al. 1997. Angiogenic and HIV-inhibitory functions of KSHV-encoded chemokines. *Science*. 278:290–294.
65. Chen, Z., P. Zhou, D.D. Ho, N.R. Landau, and P.A. Marx. 1997. Genetically divergent strains of simian immunodeficiency virus use CCR5 as a coreceptor for entry. *J. Virol*. 71: 2705–2714.
66. Edinger, A.L., A. Amedee, K. Miller, B.J. Doranz, M. Endres, M. Sharron, M. Samson, S. Lu, J.E. Clements, M. Murphey-Corb, et al. 1997. Differential utilization of CCR5 by macrophage and T cell tropic simian immunodeficiency virus strains. *Proc. Natl. Acad. Sci. USA*. 94:4005–4010.
67. Farzan, M., H. Choe, K. Martin, L. Marcon, W. Hofmann, G. Karlsson, Y. Sun, P. Barrett, N. Marchand, N. Sullivan, et al. 1997. Two orphan seven-transmembrane segment receptors which are expressed in CD4-positive cells support simian immunodeficiency virus infection. *J. Exp. Med*. 186:405–411.
68. Kirchhoff, F., S. Pohlmann, M. Hamacher, R.E. Means, T. Kraus, K. Uberla, and P. di Marzio. 1997. Simian immunodeficiency virus variants with differential T-cell and macrophage tropism use CCR5 and an unidentified cofactor expressed in CEMx174 cells for efficient entry. *J. Virol*. 71: 6509–6516.
69. Rucker, J., A.L. Edinger, M. Sharron, M. Samson, B. Lee, J.F. Berson, Y. Yi, B. Margulies, R.G. Collman, B.J. Doranz, et al. 1997. Utilization of chemokine receptors, orphan receptors, and herpesvirus-encoded receptors by diverse human and simian immunodeficiency viruses. *J. Virol*. 71: 8999–9007.